

RESEARCH

Open Access



# Obtaining HBV core protein VLPs carrying SARS-CoV-2 nucleocapsid conserved fragments as vaccine candidates

Yadira Lobaina<sup>1,2</sup>, Alexis Musacchio<sup>1,2,3</sup>, Panchao Ai<sup>1,4</sup>, Rong Chen<sup>1,4</sup>, Edith Suzarte<sup>3</sup>, Glay Chinaea<sup>3</sup>, Miaohong Zhang<sup>5</sup>, Zhiqiang Zhou<sup>5</sup>, Yaqin Lan<sup>1,4</sup>, Ricardo Silva<sup>6</sup>, Gerardo Guillén<sup>3</sup>, Ke Yang<sup>1,4</sup>, Wen Li<sup>1,4\*</sup>, Yasser Perera<sup>1,2,3\*</sup> and Lisset Hermida<sup>1,4,6\*</sup>

## Abstract

The Hepatitis B core antigen (HBcAg) has been used as a carrier of several heterologous protein fragments based on its capacity to form virus-like particles (VLPs) and to activate innate and adaptive immune responses. In the present work, two chimeric proteins were designed as potential pancorona vaccine candidates, comprising the N- or C-terminal domain of SARS-CoV-2 nucleocapsid (N) protein fused to HBcAg. The recombinant proteins, obtained in *E. coli*, were named CN-1 and CND-1, respectively. The final protein preparations were able to form 10–25 nm particles, visualized by TEM. Both proteins were recognized by sera from COVID-19 convalescent donors; however, the antigenicity of CND-1 tends to be higher. The immunogenicity of both proteins was studied in Balb/C mice by intranasal route without adjuvant. After three doses, only CND-1 elicited a positive immune response, systemic and mucosal, against SARS-CoV-2 N protein. CND-1 was evaluated in a second experiment mixed with the CpG ODN-39 M as nasal adjuvant. The induced anti-N immunity was significantly enhanced, and the antibodies generated were cross-reactive with N protein from Omicron variant, and SARS-CoV-1. Also, an anti-N broad cellular immune response was detected in spleen, by IFN- $\gamma$  ELISpot. The nasal formulation composed by CND-1 and ODN-39 M constitutes an attractive component for a second generation coronavirus vaccine, increasing the scope of S protein-based vaccines, by inducing mucosal immunity and systemic broad humoral and cellular responses against Sarbecovirus N protein.

**Keywords** HBcAg, Nucleocapsid, SARS-CoV-2, Chimeric proteins, Pancorona vaccine, Intranasal

## \*Correspondence:

Wen Li  
liwen@cbbjic.com  
Yasser Perera  
ypereranegrin@cbbjic.com  
Lisset Hermida  
lhermida@oc.biocubafarma.cu

<sup>1</sup> Research Department, China-Cuba Biotechnology Joint Innovation Center (CCBJIC) Lengshuitan District, Yongzhou City 425000, Hunan, China

<sup>2</sup> R&D Department, Yongzhou Zhong Gu Biotechnology Co., Ltd., Yangjiaqiao Street, Lengshuitan District, Yongzhou City 425000, Hunan, China

<sup>3</sup> Research Department, Center for Genetic Engineering and Biotechnology (CIGB), 10600 Havana, Cuba

<sup>4</sup> Yongzhou Development and Construction Investment Co. Ltd. (YDCI), Yongzhou Economic and Technological Development Zone, Changfeng Industry Park, No. 1 Liebao Road, Lengshuitan District, Yongzhou City, Hunan Province, China

<sup>5</sup> Hunan PRIMA Drug Research Center Co., Ltd., National Liuyang Economic and Technological Development Zone, 123 Kangtian Road, Changsha City, Hunan, China

<sup>6</sup> Science and Innovation Directorate, BioCubaFarma, Independence Avenue, No. 8126, Corner 100 Street, 10800 Havana, Cuba



© The Author(s) 2024. **Open Access** This article is licensed under a Creative Commons Attribution-NonCommercial-NoDerivatives 4.0 International License, which permits any non-commercial use, sharing, distribution and reproduction in any medium or format, as long as you give appropriate credit to the original author(s) and the source, provide a link to the Creative Commons licence, and indicate if you modified the licensed material. You do not have permission under this licence to share adapted material derived from this article or parts of it. The images or other third party material in this article are included in the article's Creative Commons licence, unless indicated otherwise in a credit line to the material. If material is not included in the article's Creative Commons licence and your intended use is not permitted by statutory regulation or exceeds the permitted use, you will need to obtain permission directly from the copyright holder. To view a copy of this licence, visit <http://creativecommons.org/licenses/by-nc-nd/4.0/>.

## Introduction

The Hepatitis B core (HBcAg) is one of the main structural antigens of hepatitis B virus (HBV) and constitutes a potent immunogen for humans and animals [1]. The extremely high immunogenicity of HBcAg can be explained by its particulate nature and its capacity to function as both T-cell-independent and T-cell-dependent antigen [2]. The natural HBcAg is assembled in particles of approximately 30 nm with icosahedral geometry composed by 120 dimer of the viral capsid protein [3]. The repetitive motifs and the protuberances in the HBcAg particles surface confer the unique ability to bind and activate a high frequency of naive human and murine B cells [4, 5]. HBcAg-specific B cells from unprimed mice are able to take up, process and present HBcAg to naive T-helper cells *in vivo* 10<sup>5</sup> times more efficiently than classical antigen presenting cells (APCs) [2]. The full length HBcAg, when is obtained as a recombinant protein in *E. coli*, retains its capacity to form virus-like particles (VLPs), able to encapsulate bacterial nucleic acid (mainly RNA) which confers potent Th1 adjuvant properties [6, 7].

The HBcAg has been widely used in preclinical studies as carrier of heterologous epitopes forming chimeric proteins [8–14]. The most frequently used site for heterologous insertion has been the immunodominant *c/e1* epitope, located in the center of the HBc primary sequence, which comprises a solvent-exposed loop that tolerates insertions of flexible peptide sequences [9, 10]. Several data are available about the evaluation of such chimeric constructs in animal models [10, 11]. It has been demonstrated that a heterologous sequence inserted into this internal loop is significantly more immunogenic than such fragment in the context of its native protein [12]. Nevertheless, due to the insertion in the loop implies structural constraints (length and particular conformation) of the heterologous motif, the N and C terminus fusion sites has been also explored with successful results [13, 14].

In the present work two recombinant chimeric proteins including two fragments from SARS-CoV-2 nucleocapsid (N) protein fused to the C-terminus of HBcAg were designed and obtained. N protein is a conserved molecule among coronaviruses, which has emerged as an attractive antigen to be included in novel generation of pan-coronavirus vaccines [15]. The study published by Matchett et al., 2021, demonstrated that N protein, presented in the Ad5 platform, protected mice against SARS-CoV-2 challenge [16]. Dangi et al., 2021, also proved that the addition of N protein in a spike vaccine formulation, improved distal protection in mouse brain [17].

The two chimeric proteins, named CN-1 and CND-1, were obtained as recombinant proteins in *E. coli*,

carrying fragments of SARS-CoV-2 N-terminal domain (NTD) (139 aa length) and C-terminal dimerization domain (CTD) (123 aa length), respectively. After the purification processes, preparations with more than 90% of purity were obtained and the presence of spherical particles of 10–25 nm were visualized by transmission electron microscopy (TEM). The antigenicity of both proteins was confirmed using a panel of SARS-CoV-2 convalescent's sera and immunogenicity studies by intranasal route in Balb/C mice were done. CND-1 showed a higher antigenicity, and accordingly, it was also the most immunogenic. The immune response generated by intranasal administration of CND-1 protein was improved when the ODN-39 M was added as adjuvant in the formulation. Importantly, the induced systemic humoral and cellular immune response was cross-reactive until SARS-CoV-1 level.

## Materials and methods

### Biological and synthetic reagents

*Escherichia coli* BL21 (DE3): F<sup>-</sup> ompT gal dcm lonhdsSB(rB<sup>-</sup> mB<sup>-</sup>) k(DE3 [lacI lacUV5-T7 gene 1 ind1 sam7 nin5]) was used for gene expression [18]. For plasmid propagation, *E. coli* strain XL1-blue [F<sup>+</sup>::Tn10 proA<sub>p</sub>B<sub>p</sub> lacIq D(lacZ)M15/recA1 endA1gyrA96(NaI<sup>r</sup>) thi hsdR17(rk m<sub>p</sub>k) supE44 relA1 lac) was employed [19].

For the evaluation of animal samples, the following recombinant antigens were purchased from Sino Biological (China). N proteins from: SARS-CoV-2 Delta (40588-V07E29), and Omicron (40588-V07E34) variants; SARS-CoV-1 (40143-V08B), MERS-CoV (40068-V08B). In addition, the peptide N<sub>351–365</sub> from SARS-CoV-2 (ILLNKHIDAYKTFPP) was synthesized with ≥ 97% purity by Zhejiang Peptides Biotech (China).

The ODN-39 M, a 39 mer, whole phosphodiester backbone CpG ODN (5'-ATC GAC TCT CGA GCG TTC TCG GGG GAC GAT CGT CGG GGG-3'), was synthesized by Sangon Biotech (China).

To evaluate the protein antigenicity the following antibody reagents were used. The anti-SARS-CoV-2 nucleocapsid polyclonal antibody (40588-T62) was purchased from Sino Biologicals (China). A monoclonal antibody anti-HBcAg (ab8637) was purchased from Abcam (USA). A panel of human sera from COVID-19 convalescent (N=27) and negative (N=10) donors were collected as part of a study approved by the Institutional Ethics Committee from The Eighth People's Hospital of Dongguan (Guangdong Province, China). Informed written consent was obtained from each participant. The study description was already reported [20].

### Obtaining of the chimeric constructs CN-1 and CND-1

The following chimeric genes were chemically synthesized:

CN-1: Truncated HBcAg core (1–149)+linker (GSSGGSSG)+N fragment (40–179) from SARS-CoV-2 (Delta variant).

CND-1: Truncated HBcAg core (1–149)+linker (GSGGSG)+N fragment (248–371) from SARS-CoV-2 (Delta variant).

Each chimeric gene was amplified by polymerase chain reaction (PCR) using the corresponding primers. The amplified band was purified and cloned into pGEM-T Easy Vector (Promega, USA). Positive clones were tested by restriction analysis, and sequencing. Each recombinant fragment was then cloned into pET28a plasmid. Positive clones were identified by restriction analysis and defined as pCN-1 and pCND-1.

The *E. coli* strain BL21 (DE3) was transformed with each recombinant plasmid by electroporation. Each clone was later inoculated, at 0.05 of Optical Density (OD), in ZY medium supplemented with Kanamycin (50 µg/ml) and let to grow for 18 h at 28 °C and 170 rpm-min (THZ-300, Blue Pard Inst, China).

### Purification processes of CN-1 and CND-1

For both proteins, CN-1 and CND-1, a similar purification protocol was implemented, with some modifications.

The transformed *E. coli* was grown during 18 h under the conditions described above, and the biomass was harvested by centrifugation at 5 000×g for 15 min at 4 °C. For cell disruption, 0.5 g of cells were resuspended in 50 mL of TE buffer (0.05 M Tris-HCl, 5 mM EDTA, pH 9.0) and treated at 4 °C, with 20 cycles (30 s with 30 s rest) in a ultrasonic machine (FS-200 T, Shanghai Sonxi US Inst, China), with 50% power rate and 20.3 kHz frequency. The resultant sample was centrifuged at 10, 000×g for 15 min at 4 °C. The supernatant was collected and filtered throughout 0.45 µm for subsequent purification steps.

As a high resolution step, the ion exchange chromatography was selected based on the particular features of the HBcAg. A volume of 20 mL from the biomass disruption soluble fraction was ½ diluted with TE buffer and applied into Q Sepharose and SP Sepharose -fast flow ion exchangers (Cytiva, Sweden) connected in tandem, and previously equilibrated with TE buffer. The loading volume of the sample was 10% and the employed flow rate was 3 cm/h. After application, columns were separated, washed independently with TE buffer and the bound proteins to SP Sepharose fast flow matrix eluted with 0.1 M NaCl step gradient. The Q Sepharose fast flow matrix was employed to remove most of the protein and DNA

contaminants present on the sample while CN-1 protein was eluted from the SP Sepharose fast flow matrix with high purity. The CN-1 protein fraction was collected at 0.3 M NaCl.

Gel filtration chromatography was used for final purification step. Sephacryl S-200 HR matrix (Cytiva, Sweden) was equilibrated with 0.05 M Tris HCl, 5 mM EDTA, 0.15 M NaCl, pH 9.0, at 15 cm/h. The CN-1 fraction eluted at 0.3 M NaCl from the SP Sepharose column was applied into the gel filtration chromatography. The CN-1 protein was collected as unique peak, which was later concentrated using Amicon system (USA), filtered by 0.22 µm and stored at 4 °C.

In the case of CND-1, the protein was eluted from the SP Sepharose fast flow matrix at 0.1 M NaCl with high purity. The CND-1 fraction collected was then applied to a gel filtration chromatography following the same conditions previously described for this step. The peak corresponding to CND-1 protein was then concentrated using Amicon system (USA), filtered by 0.22 µm and stored at 4 °C.

The detection of the protein signal was followed by the absorbance at 280 nm in all steps.

### Analysis of protein samples

BCA assay (Pierce, USA), was used to determine the protein concentration in all samples. The identity of each chimeric protein was confirmed by sodium dodecyl sulphate polyacrylamide gel electrophoresis (SDS-PAGE), Western blotting and dot blotting, using specific antibodies. Protein samples were subjected to 12% of acrylamide gel. SDS-PAGE gels were stained with Coomassie blue and scanned (iBright 1500, Invitrogen). Densitometry analysis, using Image J (1.41 version) software was employed to define the percentage corresponding with the protein band of interest. In some particular cases to increase the sensibility in the visualization of slight protein bands the SDS-PAGE gel was stained using Zinc/imidazole solution. For Western blotting, protein samples were electro transferred from an acrylamide gel to a Immobilon-P membrane (Merck-Millipore, IRL), as described [21]. In turn, samples were applied directly to the membrane for dot blotting. The membrane from the two previous procedures was blocked with 5% skim milk in phosphate buffered saline (PBS) for 1 h at room temperature (RT), washed three times with – PBS—0.05% Tween solution (PBS-T). The reaction with the anti-SARS-CoV-2 N polyclonal Ab generated in rabbit (SinoBiologicals, China) at 1:2500 dilution (or anti-HBcAg mAb (Abcam, USA) 1:1000 diluted), occurred during 1 h at RT. After proper washing, the incubation of the membrane with the peroxidase-conjugated goat anti-rabbit IgG (Chemicon, USA) at a 1/300 dilution, or anti-mouse IgG-peroxidase,

respectively, occurred during 1 h at RT. Antibodies used during the whole procedure were diluted in 1% skim milk in PBS-T. Afterwards, upon membrane washing, the reaction was detected by incubation with Aminoethyl Carbazole (AEC) substrate solution (0.2 mg/ml AEC and 0.03% H<sub>2</sub>O<sub>2</sub> in 50 mM NaAc solution) at RT.

#### **Visualization of capsid like particles (CLPs) by transmission electron microscopy (TEM)**

Etest company (Changsha, China) provided the specialized service of transmission electron microscopy analysis. CN-1 and CND-1 samples, at concentration of 0.25 mg/ml, were placed on a freshly glow-discharged, 400-mesh copper grid coated with Formvar and Carbon. After sample absorption and water washing, Uranyl Acetate stain was added. After 4 min of staining, grids were wick dried with Whatman no. 1 filter paper and later, during 20 min, were allowed to air dry.

The Transmission Electron Microscope HT 7800 (Hitachi, Japan) with an acceleration voltage of 120 kV and three magnifications: 25 000 x, 50 000 x, and 100 000 x, was the equipment used for sample visualization. For each sample, eight different fields were analyzed. The Image J software (Maryland, USA) was used to estimate the average particle size.

#### **Characterization of CN-1 and CND-1 proteins, by ELISA, using human sera positive to SARS-CoV-2**

Ninety-six-well high-binding polystyrene plates (Costar, USA) were coated with 3 µg/mL of each protein (CN-1 and CND-1), in sodium carbonate-sodium bicarbonate buffer, and incubated overnight at 4 °C. Unspecific binding of the antibodies was avoided by blocking with 5% skim milk (Oxoid, UK) 1 h at 37 °C. After five times washing with PBS-T, 100 µL of diluted serum sample in 2% skim milk -PBS-T were added and incubated for 2 h at 37 °C. After washing five times with PBS-T, bound antibodies were detected with a goat anti-human IgG antibody conjugated to horseradish peroxidase (Sigma-Aldrich, Germany) at 1:20,000 dilution. After incubation for 1 h at 37 °C and five PBS-T washes, 100 µL of OPD substrate solution (Sigma-Aldrich, Germany) were added to each well and the mixture was incubated for 10 min in the dark at RT. The reaction was stopped by adding 0.2N Sulphuric Acid, and the optical density (O.D) at 492 nm was measured in a multiplate reader (FilterMax F3, Molecular Devices, USA). The data is represented as O.D measures.

#### **Animal experiments in Balb/C mice**

Beijing Vital River Laboratory Animal Technology Co., Ltd, and Hunan Prima Drug Research Center Co., Ltd, conducted the mice experiments. Both animal facilities

complied with the national standard of the People's Republic of China GB14925-2010. Each experimental protocol was subjected to analysis and approval by the Institutional Animal Care and Use Committee.

Three doses of immunogens were intranasally (in) inoculated in each group of mice (N=5 or N=6), according to the defined design. Ten µg of each protein (CN-1 or CND-1) was administered per animal. All the immunogens were dissolved in sterile PBS in a volume of 50 µL. As negative controls, placebo groups were included in the experiments.

In the first animal study, mice were distributed in three groups of six animals each. Group 1 was inoculated with CN-1 protein, Group 2 received CND-1 protein, and PBS was administered to the Group 3, as negative control. The administration schedule was 0, 15 and 30 days. Twenty-seven days after the last dose, mice were sacrificed.

For the other study, mice were distributed in three groups of five animals each. Groups 1 and 2 received CND-1 protein and CND-1+15ug ODN-39 M, respectively. Group 3 corresponded to the Placebo group, similar to the previous study. The administration schedule was 0, 7 and 21 days. Thirty days after the last dose, mice were sacrificed.

Three different samples were obtained at the indicated time points: sera, spleens, and bronchoalveolar fluid (BALF).

#### **Determination of antibody response by ELISA**

The Ab response in sera and BALF was measured by anti-IgG, IgG subclasses, and, -IgA ELISAs [22]. Briefly, 96 well high-binding plates (Costar, USA) were coated with N or HBcAg protein (3 µg/mL) and blocked with 2% skim milk solution. Samples were evaluated in duplicates starting from 1/100 dilution of sera. BALF were tested without dilution. Specific horseradish peroxidase conjugates (Sigma, USA) and OPD (Sigma, USA)/hydrogen peroxide substrate solution were employed. The reaction was stopped using 2 N Sulphuric acid and multiplate reader (FilterMax F3, Molecular Devices, USA) was used to measure O.D at 492 nm. In the graphics corresponding with sera Ab response log<sub>10</sub> titers are represented. The arbitrary units of titers were calculated by plotting the O.D values obtained for each sample in a standard curve (hyper-immune serum of known titer). The positivity cut-off was established as 2 times the average of O.D obtained for a pre-immune sera pool. In the case of BALF, the antibody response was represented as O.D at 492 nm.

#### **Evaluation of cell-mediated immunity by IFN-γ ELISpot**

The Mouse IFN-γ ELISpot antibody pair (Mabtech, Sweden) was employed to perform the ELISpot assay. Splenocytes (from five mice per group) were isolated in

RPMI culture medium (Gibco, US) and processed individualized. In the case of Placebo group, splenocytes were processed as a pooled sample of five animals. Duplicates cultures ( $5 \times 10^5$  and  $1 \times 10^5$  splenocytes per well) were incubated for 48 h at 37 °C and 5% CO<sub>2</sub>, in a 96 well round-bottom culture plate (Costar, USA) with 10 µg/mL of each stimulating agent: N<sub>351–365</sub> peptide, N proteins, and Concanavalin A (ConA). Control wells of cells without stimulus (medium) were included for all samples. After the incubation period, the whole content of each culture plate was transferred to ELISpot pre-coated plates (Merck-Millipore, USA) and incubated for 16–20 h at 37 °C and 5% CO<sub>2</sub>. The following steps were performed according to the manufacturer's recommendation. For spot counting, a stereoscopic microscope (AmScope SM-1T5Z, USA) coupled to a digital camera was employed.

### Statistical methods and analysis

The GraphPad Prism version 5.00 statistical software (Graph-Pad Software, USA) was used for all the analyses. To reach a normal distribution, antibody titers were transformed to log<sub>10</sub>. For the non sero-converting sera, an arbitrary titer of 1:50 was assigned for statistical processing. As a parametric test, the One-way Anova test followed by a Tukey's post-test was selected for multiple group comparisons. For the non-parametric multiple comparisons, the Kruskal Wallis test and Dunns post-tests was used. P values were considered as: ns,  $p > 0.05$ ; \*,  $p < 0.05$ ; \*\*,  $p < 0.01$ ; \*\*\*,  $p < 0.001$ .

## Results

### Obtaining of CN-1 and CND-1 constructs

Figure 1a represents the design of the two chimeric proteins, CN-1 and CND-1. The DNA sequence corresponding to each chimeric gene was cloned into the PET-28a vector. *E. coli* BL21 (DE3) was transformed with each recombinant plasmid and grown in ZY auto-induction medium. An overexpressed band of molecular weight (MW) around 32.7 kDa and 31.1 kDa, matching with the theoretical size of the CN-1 and CND-1 proteins respectively, was detected by SDS-PAGE, accounting for the 5% of the total cellular proteins (Fig. 1b and c). In addition,

the identity was confirmed by western blot assay. Each band was immune-identified with anti-SARS-CoV-2 nucleocapsid polyclonal Ab (Fig. 1b and c, right panel).

After expression of each recombinant construct, the biomass from the bacterial culture was disrupted. Under established conditions, both chimeric proteins were mainly associated to the cell disruption soluble fraction (Fig. 1d and e). The subsequent high resolution purification steps were similar for both proteins (Fig. 1f), with slight modifications. In general, a sample for each disruption process (for CN-1 and CND-1) was applied into two ionic exchange chromatographies coupled in tandem (Q and SP Sepharose fast flow). Contaminants were attached to the first anion exchange matrix whereas each target protein was bound to the cation one. Since the elution from the SP Sepharose was conducted by step gradient, additional contaminants were removed at low molarities of NaCl. The CN-1 and CND-1 proteins were eluted at 0.3 M and 0.1 M NaCl, respectively, with a high level of purity. As final polishing purification step, the gel filtration chromatography was introduced using Sephacryl S-200 HR. Both proteins were obtained with more than 90% of purity and were properly immune-identified by both, polyclonal Abs anti-SARS-CoV-2 N and the anti-HBcAg Mab (Fig. 1g, h and i).

The characterization by SDS-PAGE and Western blotting of each purified protein, under native conditions, is shown in Fig. 1j and k. Interestingly, aggregated forms of high MW were visualized for both proteins although the highest MW species were only visualized in the CND-1 sample.

### Visualization of capsid like particles

TEM was selected as the analytical method to define the ability of each chimeric protein to form CLPs. Three pictures, visualized with three magnification factors are represented in Fig. 2. Particles with similar spherical morphology were detected in the samples of the two chimeric proteins. The particles visualized for CND-1 and CN-1 samples have an average size of 12.2 nm and 19.4 nm, respectively. On the other hand, the vaccine preparation composed by CND-1 mixed with ODN-39 M

(See figure on next page.)

**Fig. 1** Expression, purification and characterization of CN-1 and CND-1 proteins (a) Simplified diagram of CN-1 and CND-1 constructs. Expression analysis, by SDS-PAGE and Western blotting using anti-SARS-CoV-2 nucleocapsid (N) polyclonal Ab, of samples from CN-1 (b) and CND-1 (c) 1: MW molecular weight marker, 2: Cell extract of *E. coli* BL21 (DE3) transformed with each recombinant plasmid. Analysis of the disruption process by SDS-PAGE, of CN-1 (d) and CND-1 (e) samples. 1: MW marker, 2: Cell extract of *E. coli* BL21 (DE3) transformed with each recombinant plasmid, 3: Supernatant after disruption, 4: Pellet after disruption. (f) Diagram of the purification process. (g) Dot blotting of purified samples of CN-1 and CND-1 proteins, using 1: anti-HBcAg mAb and 2: anti-N polyclonal Ab. Analysis by SDS-PAGE of purified proteins CN-1 (h) and CND-1 (i) 1: MW marker, 2: Sample of elution from Sephacryl S-200 HR. (j) Analysis by SDS-PAGE under native conditions, and Western blot using polyclonal anti-N Abs (k), of samples of each purified protein 1: MW marker, 2: CN-1, 3: CND-1. All SDS-PAGE gels were stained with Coomassie blue, except 1j that was stained using Zinc/imidazole

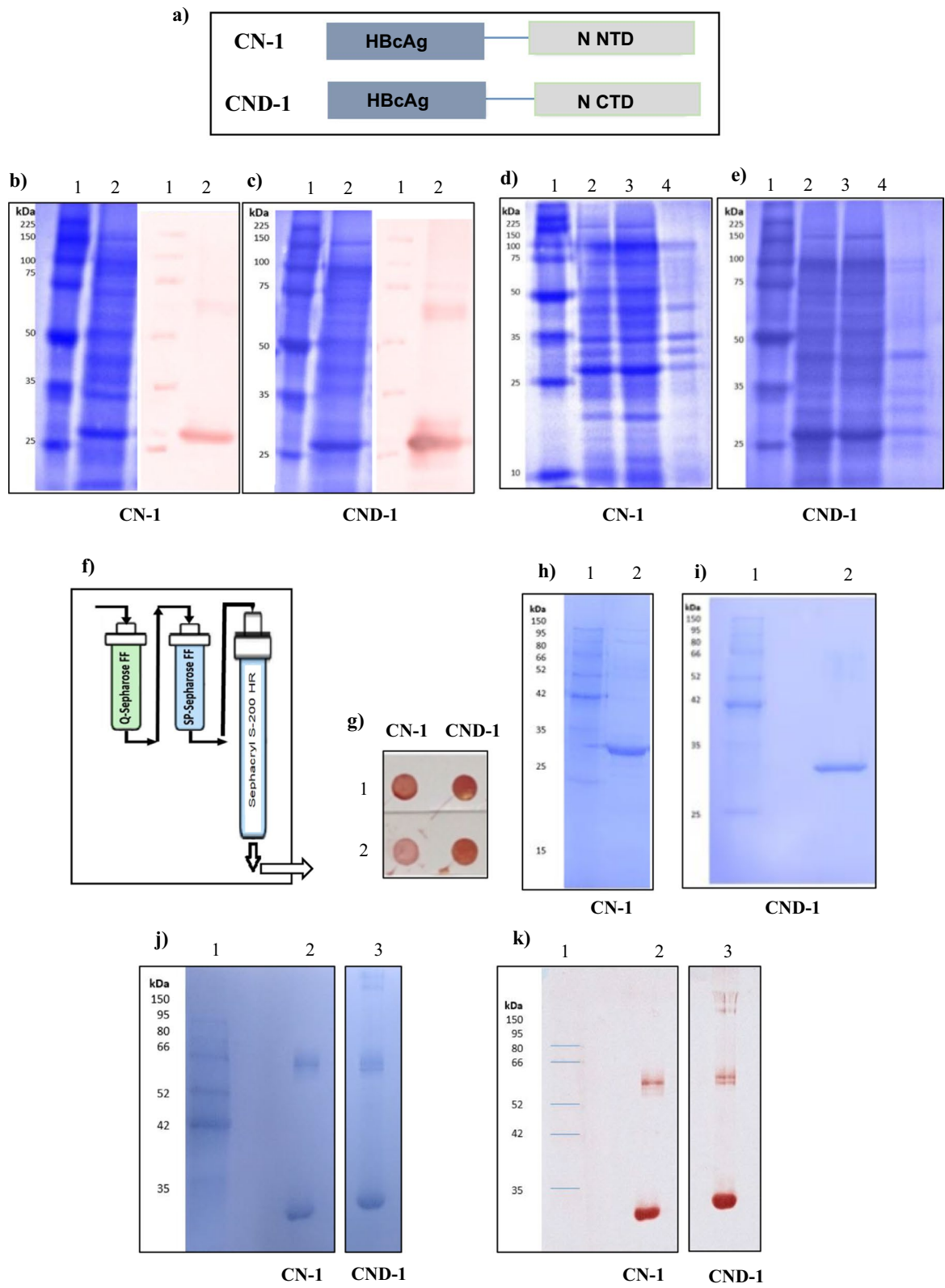


**Fig. 1** (See legend on previous page.)

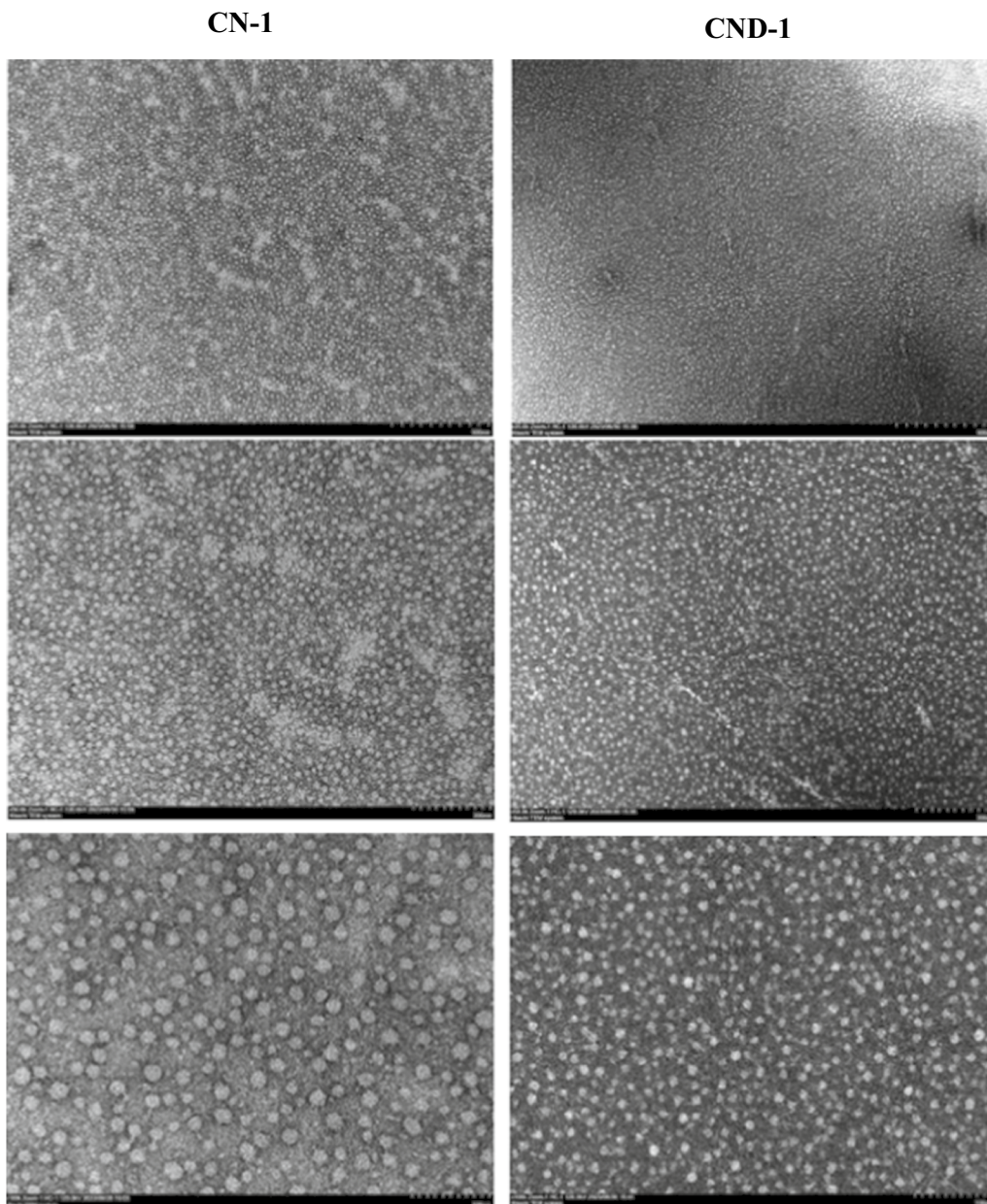


**Fig. 2** TEM using HT7800 Hitachi microscope. Three pictures corresponding with 25 000, 50 000 and 100 000 $\times$  magnifications, respectively, are shown. Left panel: CN-1, Right panel: CND-1

adjuvant showed a similar pattern of particles with mean size of 15.2 nm (data not shown). No clear evidences of dimeric or aggregated structures were observed in the evaluated samples.

#### **Recognition of CN-1 and CND-1 by SARS-CoV-2 positive sera**

A panel of human sera (positive and negative against SARS-CoV-2 antigens) was used to determine the

recognition of the chimeric proteins CN-1 and CND-1. The Fig. 3 represents the results obtained. Both recombinant proteins were recognized by the positive human sera although the recognition of CN-1 tended to be lower. Furthermore, three sera samples belonging to the negative donors group showed a positive recognition for both chimeric proteins. These specific sera samples were additionally tested against HBcAg, by ELISA, and showed a positive recognition to hepatitis B capsid protein (data not shown).

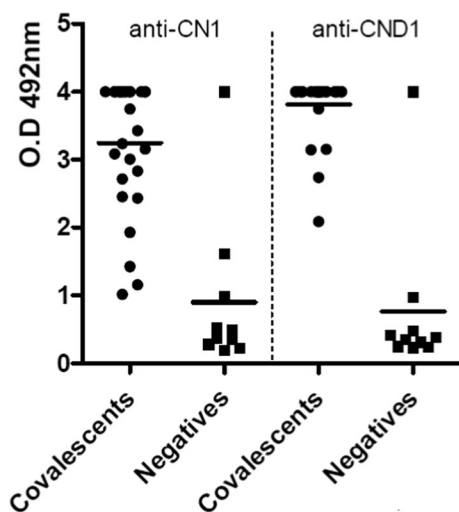


**Fig. 3** Recognition of CN-1 (left panel) and CND-1 (right panel) recombinant chimeric proteins by SARS-CoV-2 convalescent human sera. Data is presented as O.D.<sub>492nm</sub> values from each individual serum. Horizontal bar represents the mean of the group in each case. (Block circle) Convalescent and (block square) negative sera

#### CN-1 and CND-1 immunogenicity in Balb/C mice by intranasal route

A mice experiment was conducted to explore the immunogenicity of each chimeric protein administered by intranasal route. Three doses, using 10 µg of each protein per dose, were administered without adjuvant (Fig. 4a). In sera, only the group receiving the CND-1 protein elicited an IgG antibody (Ab) response specific against N protein from SARS-CoV-2 and HBcAg, as shown in Fig. 4b and d respectively. Accordingly, a similar pattern was obtained when the specific IgA Abs were measured in BALF samples (Fig. 4c and e).

To test the CMI, spleen cells were *in vitro* stimulated with the conserved peptide N<sub>351–365</sub> and the N protein from SARS-CoV-2. The frequency of IFN-γ secreting cells was measured by ELISpot assay. According to the humoral immune response, mice receiving CND-1 by intranasal route exhibited a positive response against the peptide N<sub>351–365</sub> (Fig. 4f). Of note, no response was detected for any group upon stimulation with N protein from SARS-CoV-2 (data not shown).

#### Immunogenicity of the mixture CND-1 + ODN-39 M

Based on the nasal immunogenicity results previously described, CND-1 protein was selected to combine with the mucosal adjuvant ODN-39 M as a potential nasal vaccine candidate. Three doses of each immunogen (10 µg CND-1 alone, or 10 µg CND-1 + 15 µg ODN-39 M) were intranasally administered (Fig. 5a).

As expected, the group receiving CND-1 + ODN-39 M elicited high levels of IgG Abs in sera against N protein from SARS-CoV-2, with statistical differences compared to titers induced in the group inoculated with CND-1 without adjuvant (Fig. 5b). In turn, upon IgG subclass pattern analysis, similar and high levels of IgG1 and IgG2a were elicited in animals of the group receiving the protein with adjuvant, indicating the induction of a balanced Th1/Th2 pattern of response against N protein from SARS-CoV-2 (Fig. 5c). On the other hand, similar to the IgG Abs in sera, the levels of mucosal IgA against N protein from SARS-CoV-2 measured in BALF were higher in the group receiving CND-1 with adjuvant ( $p < 0.05$ ) (Fig. 5d).

Furthermore, the HBcAg-specific antibody response exhibited a similar behavior. The IgG levels in sera and IgA levels in BALF, against the carrier protein, were higher in the group receiving the combination of CND-1 + ODN-39 M showing statistical differences compared to the group receiving the chimeric protein without adjuvant (Fig. 5e and f).

Samples were additionally tested against N proteins from SARS-CoV-2 Omicron variant, SARS-CoV-1 and MERS-CoV so as to determine the scope of the systemic humoral immune response. As shown in Fig. 6a, high levels of IgG were detected against N proteins from SARS-CoV-2 Omicron variant, and SARS-CoV-1, for the group immunized with the adjuvated preparation, whereas no response was obtained against N protein from MERS-CoV.

Finally, to test the CMI, spleen cells were *in vitro* stimulated with the conserved peptide N<sub>351–365</sub> and the N protein from SARS-CoV-2 Delta and Omicron variants, and the N protein from SARS-CoV-1. In line with the humoral immune response generated, mice intranasally inoculated with the mixture CND-1 + ODN-39 M exhibited a clear trend to develop a higher response (Fig. 6b). The 100% of animals in this group were positive against the peptide N<sub>351–365</sub>, and the N protein from SARS-CoV-2 Delta and Omicron variants. On the other hand, the IFN-γ response specific against the N protein from SARS-CoV-1 was positive in two out of 5 animals.

#### Discussion

In the present work the N protein from SARS-CoV-2 (Delta strain) was selected as the source of the heterologous fragments to be fused to HBcAg since it is a conserved coronavirus antigen and target of CMI response in humans [23]. Accordingly, several TCD4<sup>+</sup> and TCD8<sup>+</sup> epitopes have been mapped on it [24–26]. Particularly, the two regions selected for fusing to HBcAg, NTD and CTD fragments, exhibit high percentage of identity at sarbecovirus level (>90%) and their lengths and

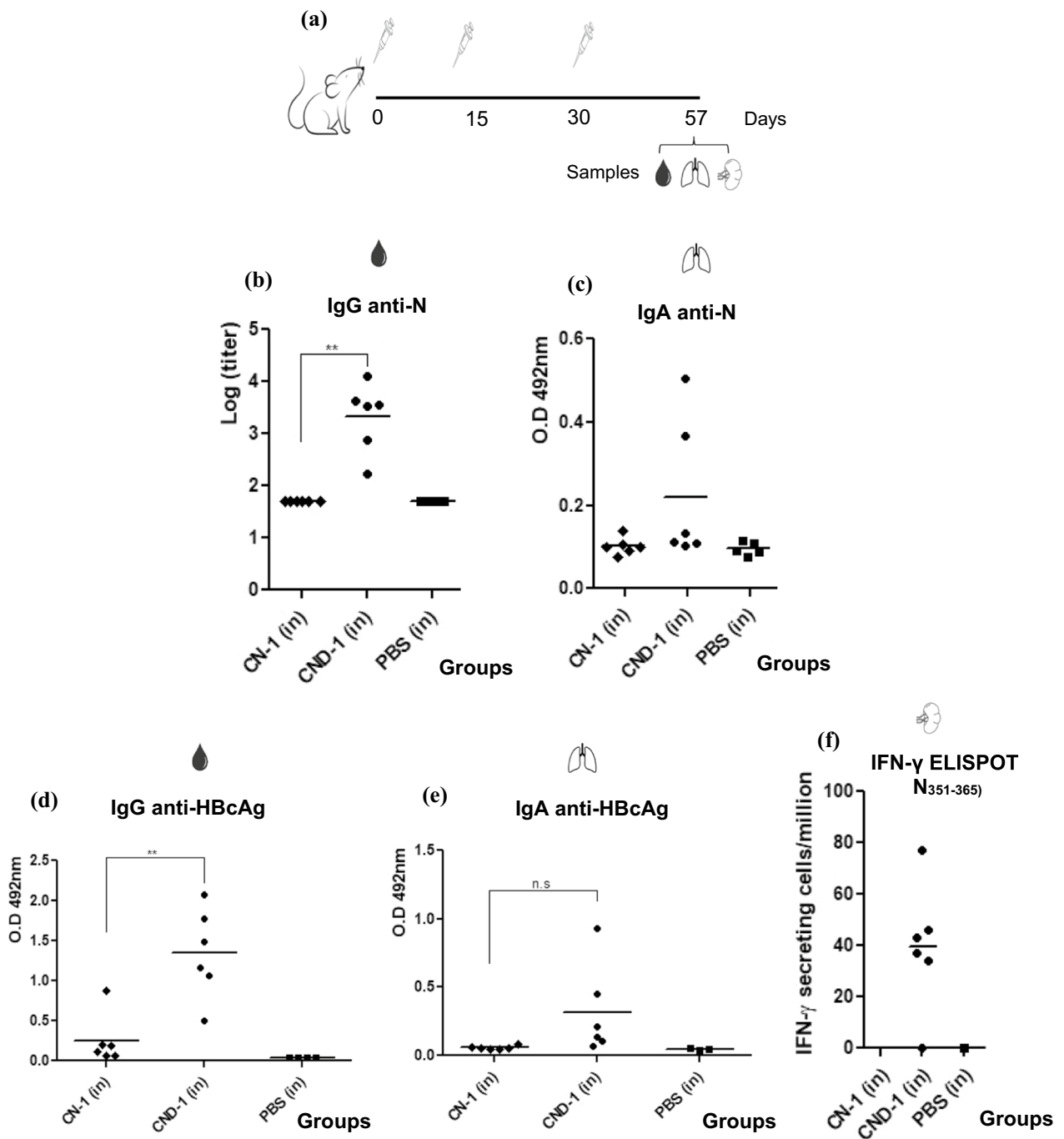


**Fig. 4** Immunogenicity of CN-1 and CND-1 proteins, in Balb/C mice, administered by intranasal (in) route. Six- to eight-week-old mice were immunized with three doses of each formulation: Group 1: CN-1, Group 2: CND-1, Group 3: PBS. Twenty-seven days after the third immunization, mice were sacrificed. Antibody responses in the serum and bronchoalveolar lavage fluid (BALF) as well as CMI in spleen, were evaluated. **a** Diagram of immunization. Humoral immune response measured by ELISA, anti-N protein from SARS-CoV-2, **b** IgG in sera, **c** IgA in BALF; anti-HBcAg **d** IgG in sera and **e** IgA in BALFs. Data of IgG are represented as log10 of the titers. Data from IgA are expressed as O.D.<sub>492nm</sub>. **f** Frequency of IFN-γ secreting cells, by ELISpot, in splenocytes after in vitro stimulation with the conserved peptide N<sub>351-365</sub>. Graph shows the response of individual mice. In all graphics the horizontal bar represents the mean value of the group. The statistical analysis was done by One-Way Anova followed of Tukey's multiple comparison test. \*\* $p < 0.01$ , \*\*\* $p < 0.001$

structures are compatible to be fused at the C-terminus site of the HBcAg. Despite the most used carrier site in the HBcAg is the immunodominant c/e1 epitope, we discard it due to its lack of compatibility with the structure of the N fragments. In turn, the length of each N selected fragment (139 aa and 123 aa for CN-1 and CND-1, respectively) inserted in such site would affect the capacity of the resultant chimeric protein to form capsid-like particles, a crucial feature of the HBcAg which correlates with its high immunogenicity by intranasal route [27]

As a first signal of proper conformation, both chimeric proteins (CN-1 and CND-1) were mainly associated to the soluble fraction after biomass disruption. In addition, a scale up purification process, without using chaotropic agents, could be established for each construct. After analysis by TEM, particles of 10–20 nm were visualized, indicating that the fusion of the heterologous fragments from SARS-CoV-2 N protein does not limit the particle formation ability of the HBcAg. This result is in accordance to several reports describing the formation of CLPs upon fusion of large heterologous cargoes at the C terminus of HBcAg, such as the Dom III of the envelope protein from Zika virus (100 aa), a region from *Staphylococcus aureus* nuclease (163aa), and the Hepatitis C core fragment (91aa) [14, 28, 29]. In general, the CLPs average size obtained here for both chimeric proteins is on the range, but a little lower to the previously reported for the full-length HBcAg antigen. It is widely known that the full length HBcAg (183 aas), expressed as recombinant protein in *E. coli*, is able to form VLPs with a size ranging between 25 and 30 nm [30]. However, these VLPs show an electro-dense core, corresponding with the presence of encapsulated bacterial nucleic acids, which confers the extremely high immunogenicity of HBc particles. In our work we selected the truncated HBcAg variant (149 aas) as carrier for the N fragments, considering the remaining capacity of this variant to form CLPs structures and also the big size of the cargoes. In this case the presence of associated bacterial nucleic acid, after the obtaining of the chimeric proteins in *E. coli*, was not observed for none of the proteins as it is shown in the TEM photographs and also after agarose gel electrophoresis analysis (data not shown). The truncated HBcAg lacks the

Arginine-rich domain (naturally located at the C-terminal end) which is the main responsible for the nucleic acid binding during the natural DNA encapsulating role of the HBV nucleocapsid protein [31]. In the design of the CN-1 and CND-1 chimeric proteins we hypothesized that the SARS-CoV-2 N fragments included could contribute to the nucleic acid binding effect, considering the reported RNA binding capacity of these domains [32]. However, the final outcome didn't show evidences of bacterial nucleic acid association in the purified preparations of both chimeric proteins. This could explain in part the lower immunogenicity observed for both antigens after intranasal administration.

On the other hand, it was interesting the tendency to a lower recognition of CN-1 protein compared with CND-1 protein, when they were tested against a panel of SARS-CoV-2 convalescent sera. This fact can be explained by the higher immunogenicity of the CTD region of SARS-CoV-2 nucleocapsid protein compared with the NTD region, or due to a better conformation obtained for the CND-1 chimeric protein. On the other hand, it was interesting the aggregation profile of both proteins, observed by SDS-PAGE and Western blot under native conditions. Both of them form species of high molecular weight though bands with the highest MW were only visualized for CND-1. It indicates that CTD region tends to form highly aggregated structures, in line with the report by Lo YS et al. 2013, where authors demonstrated the oligomerization capacity of the CTD from the human coronavirus 229E nucleocapsid protein [32].

Taking the advantage of the capacity of HBcAg to induce mucosal Abs when it is administered by intranasal route [27], as well as the relevance to induce an anti-SARS-CoV-2 broad mucosal immune response for cutting the transmission upon viral entry or at least, to decrease the infection levels in lungs, the intranasal route was selected for the evaluation of the chimeric proteins in Balb/C mice.

The results reveal the superior immunogenicity of CND-1 compared to CN-1 when they were administered by intranasal route without adjuvants. CN-1 neither induces humoral nor CMI response anti-N protein

(See figure on next page.)

**Fig. 5** Humoral immunity elicited by CND-1 alone and combined with ODN-39 M, administered by intranasal route in Balb/C mice. Six- to eight-week-old mice were immunized with three doses of each formulation: Group 1: CND-1, Group 2: CND-1 + ODN-39 M, Group 3: PBS. Thirty days after the third immunization, mice were sacrificed. Antibody responses in the serum and BALF were evaluated. **a** Diagram mouse immunization. Humoral immune response anti-N protein from SARS-CoV-2 measured by ELISA **b** IgG and **c** IgG1 and IgG2a in sera, and **d** IgA in BALFs. Humoral immune response anti-HBcAg measured by ELISA **e** IgG in sera, and **f** IgA in BALF. Data of IgG are represented as log<sub>10</sub> of the titers. Data from IgA are expressed as O.D.<sub>492nm</sub>. The horizontal bar represents the mean value. The statistical analysis was done by One-Way Anova followed of Tukey's multiple comparison test. \*\* $p < 0.01$ , \*\*\* $p < 0.001$

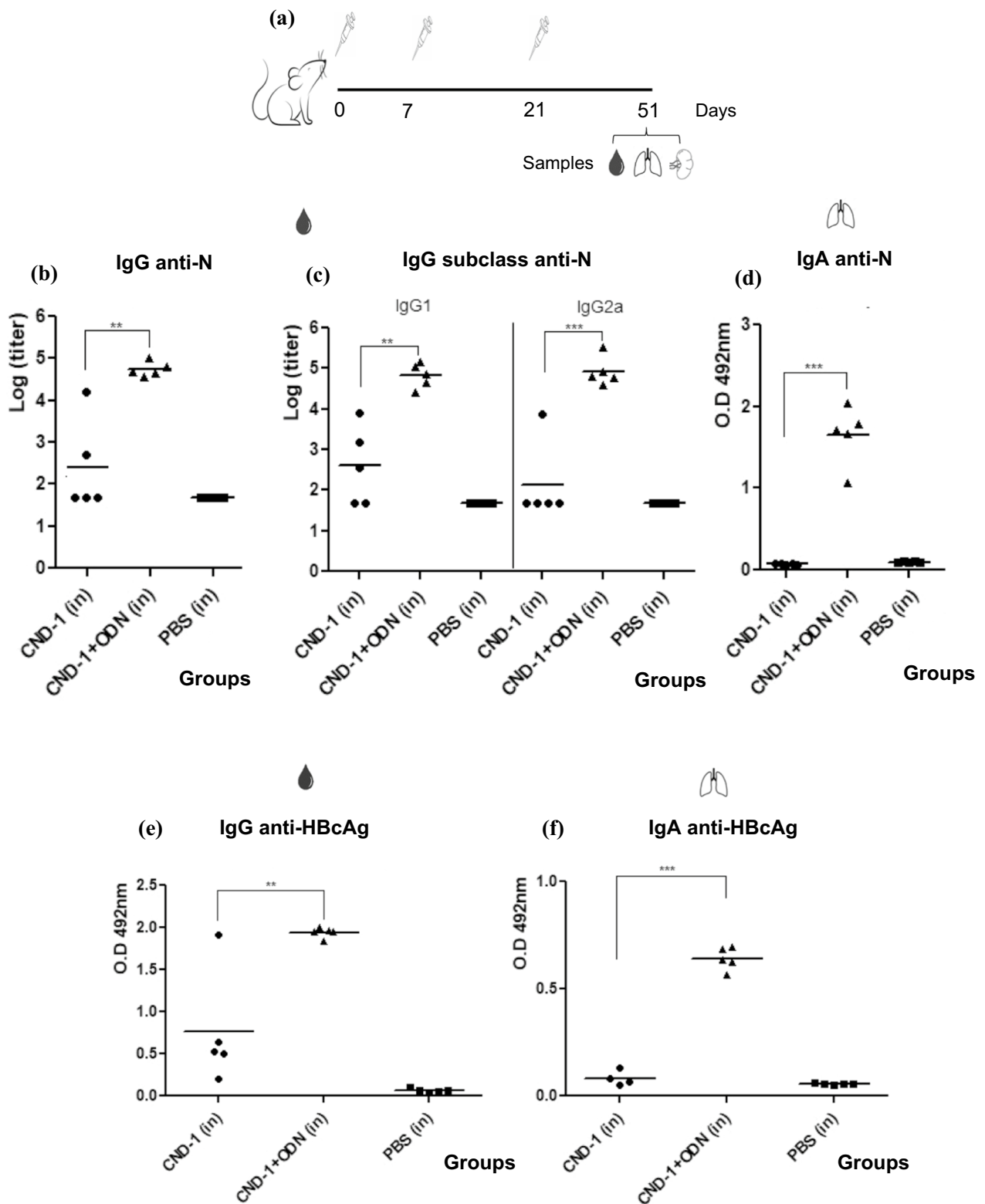


**Fig. 5** (See legend on previous page.)

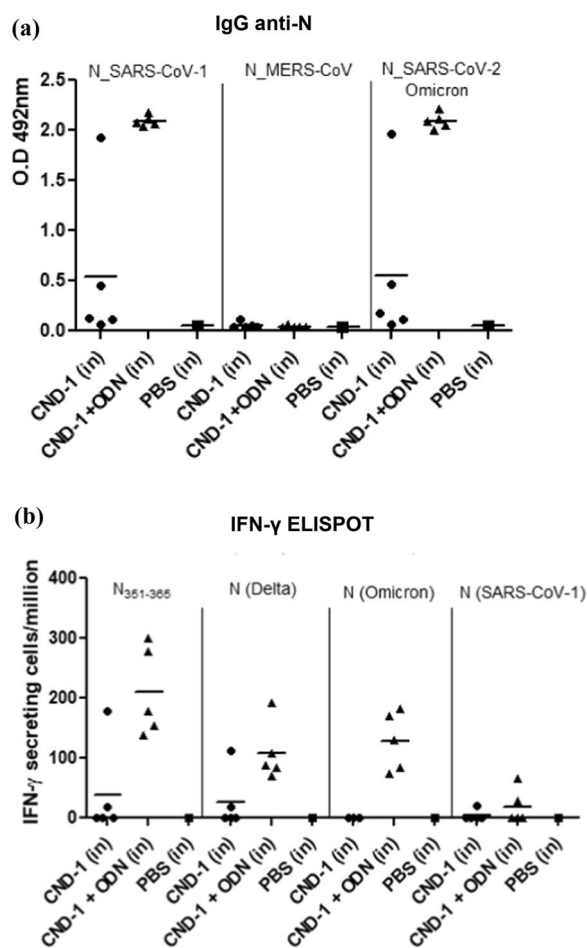


**Fig. 6** Cross-reactivity of the systemic immune response generated in Balb/C mice by the intranasal administration of CND-1 alone and combined with ODN-39 M. Thirty days after the third immunization mice were sacrificed. **a** IgG antibody response against N protein from SARS-CoV-1, MERS-CoV, and SARS-CoV-2 Omicron variant were measured by ELISA in sera at 1:100 dilution. Data are expressed as O.D values, horizontal bar represents the mean value. **b** Cell-mediated immune response. Spleens cells were isolated and in vitro stimulated with the conserved peptide N<sub>351-365</sub> and N proteins from SARS-CoV-2, Delta and Omicron variants, and SARS-CoV-1. The frequency IFN-γ secreting cells was measured by ELISpot. Square dots represent a pool of placebo samples. The horizontal bar represents the mean value for each group ( $n=5$ )

from SARS-CoV-2 under these conditions. This result is in accordance to the lower recognition of this protein by human sera and the absence of high MW aggregates by SDS-PAGE. Accordingly, none or a very low Ab response against HBcAg was obtained for CN-1. On the contrary, CND-1 was immunogenic, measured in both systemic humoral immunity and CMI against N protein from SARS-CoV-2 and the N<sub>351-365</sub> peptide, respectively. Of note, the recombinant SARS-CoV-2 N protein obtained also in *E. coli*, recently evaluated by our group, was not

able to induce such immunity in mice without adjuvant by intranasal route [33]. Results indicate that the presentation to the immune system of the CTD fragment is favored on the context of HBcAg, probably due to the highly aggregated nature of the resultant chimeric protein, and the intrinsic adjuvant properties of the HBcAg scaffold [4–7]. It is known that the presence of particulate structures or protein aggregates in the nanometric size range result better immunogens after nasal administration [34].

Despite 100% of responders were obtained in the CND-1 group by anti-N IgG ELISA in sera and ELISpot assay using the conserved T CD4+N peptide (N<sub>351-365</sub>) as stimulating agent, in BALE, only two animals exhibited IgA anti-N positive response. In turn, also by ELISpot assay, no response was detected when the N protein of SARS-CoV-2 was used as stimulating agent. Based on these results, we decided to study the inclusion of the ODN-39 M as adjuvant in the CND-1 nasal formulation. The ODN-39 M is a CpG ODN which bind to and activate Toll-like receptor 9 (TLR9) for initiating the innate immune response and consequently, enhance the adaptive immune response [35]. CpG ODNs are being evaluated in more than 100 clinical trials focused on preventing or treating allergy, infectious diseases and cancer [36]. Particularly, the ODN-39 M has been previously evaluated in combination with four different viral recombinant capsid proteins proving its adjuvant effect [33, 37–39]. In accordance, in the present work, the addition of ODN-39 M to the CND-1 protein preparation for nasal administration significantly enhanced the humoral immunity (systemic and mucosal) and systemic CMI induced against N protein from SARS-CoV-2. In turn, analyzing together the IgG subclasses results obtained in sera, and the levels of gamma-interferon secretion measured in spleen, both suggests the development of a Th1 pattern of response at systemic compartment, similar to that described for viral infections. Actually, the anti-N immunity, comprising both arms of the immune response, has been correlated with protection against coronavirus in mice, monkeys, and humans [16, 23, 40]. However, while the role of the T-cell mediated anti-N immunity is strongly documented, the contribution of nucleocapsid-specific humoral immunity remains controversial [41]. In this line, Dangi et al., 2022 [42] showed that mice receiving nucleocapsid-specific sera or mAb exhibited enhanced control of SARS-CoV-2. They demonstrated that the nucleocapsid-specific antibodies are able to elicit NK-mediated, antibody-dependent cellular cytotoxicity (ADCC) against infected cells. Accordingly, in humans, anti-N Abs have been administered to treat COVID-19 patients with promising results against the severity of the disease [43]. Furthermore, a more recent

work corroborated previous observations that nucleocapsid serostatus prior to SARS-CoV-2 breakthrough infection correlates with disease protection by showing that anti-N seropositive individuals have an increased rate of virus clearance and lower peak viral loads compared to seronegatives [44]. On the other hand, N protein is as target of cross-reactive memory T cells, which were associated to protect SARS-CoV-2 naïve contacts from infection, thereby supporting the inclusion of this protein antigen in a new vaccine generation [23].

The breath of the systemic anti-N immunity, induced by intranasal administration of the CND-1 + ODN-39 M preparation, revealed its potentiality to be considered as an attractive component of a pancorona vaccine. The humoral immune response reached cross-reactivity until SARS-CoV-1 level, whereas for CMI, high level of response was obtained when the conserved peptide N<sub>351-365</sub> was used as simulating agent. Importantly, this peptide spans a conserved region among sarbecovirus which is immunodominant in SARS-CoV-2 Balb/C infected mice. In addition, it was able to partially protect mice from SARS-CoV-2 infection when administered in the context of Venezuelan equine encephalitis replicon particles vector. This experiment provided direct evidence about the protective role of memory T-cells against the conserved peptide N<sub>351-365</sub> [45].

The homology level of SARS-CoV-2 nucleocapsid protein within the beta coronavirus genus supports the results obtained in the present work. The identity of N protein within sarbecoviruses subgenus is in the range of 87–99% whereas the identity between nucleocapsid of SARS-CoV-2 and MERS-CoV is only 48% [46]. Despite the response obtained in our mice experiments did not react with the N protein from MERS-CoV, we consider that cross-immunity at sarbecoviruses levels is very important. Currently, more than 50 SARS-related coronaviruses have been identified in 10 species of bat [47]. Bat-borne SARS-related coronaviruses are considered target of potential pandemics due to their diversity. Accordingly, Crook JM et al., 2021 expressed that the highest the probability for homologous recombination of sarbecoviruses through co-infection, the biggest the possibility of novel zoonotic emergence [48].

It is important to highlight that the immunogenicity obtained for the preparation of CND-1 + ODN-39 M, nasally administered, is similar to that generated by the recombinant N protein combined with the same adjuvant. In a previous work, the N + ODN-39 M preparation, administered by intranasal route, induced anti-N CMI response in spleen and also elicited broad humoral immunity in both, sera and lungs [33]. Nevertheless, CND-1 shows a higher nasal immunogenicity, being able to induce anti-N immune response when it

is administered without any adjuvant. Such an intrinsic response is potentiated by the inclusion of the ODN-39 M in the preparation.

Finally, since the chimeric protein CND-1 use the HBcAg as scaffold or platform, the anti-HBcAg humoral immunity was also determined. Interestingly, positive response of IgG in sera and IgA in BALF against HBcAg were enhanced after combination with ODN-39 M. It is known that the immune response against HBcAg partially contributes to the protection against HBV infection [49, 50], therefore, since CND-1 is also able to generate such anti-HB immunity, it constitutes a further advantage of this antigenic preparation. In addition, it has been recently reported the use in humans of a nasal administered preparation based on HBcAg as non-specific innate immune stimulator to preventively train the system for fight potential respiratory infections or as early prophylaxis treatment [51]. In that work the authors found that the HBcAg, when administered by nasal route, is able to increase the expression of several IFN-stimulated genes. This effect could be another advantage of the use of the CND-1 + ODN nasal vaccine preparation.

The results obtained in the present work demonstrate that the heterologous CTD fragment of N protein from SARS-CoV-2 virus can be fused to HBcAg C-terminus, without affecting its capacity of forming aggregates and CLPs. The resultant chimeric protein is immunogenic when it is administered in Balb/C mice by nasal route without adjuvants, being able to generate systemic and mucosal immune response against N and HBcAg. The nasal immunogenicity of CND-1 protein is enhanced by the addition of the mucosal adjuvant ODN-39 M. The preparation CND-1 + ODN constitutes an interesting component to be included in second generation coronavirus vaccines with broader scope, and also has potentiality to be use as booster alternative to enhance the current immunity. In addition, the strategy of employ the HBcAg as carrier for other antigens of interest, related to threatening respiratory infections, results appealing considering its particular mucosal and systemic immunity activation capacity, and the relatively easy obtaining in *E. coli*.

### Supplementary Information

The online version contains supplementary material available at <https://doi.org/10.1186/s12985-024-02583-9>.

Additional file 1.

### Acknowledgements

We acknowledge to Dr. Jiang from Guangdong Eighth People's Hospital, Guangdong Province, China, for providing the samples from COVID-19

convalescent donors. We acknowledge to Dr. Alejandro Martín for the assistance on the Molecular biology work.

#### Author contributions

Conceptualization, L.H., Y.Lobaina., G.C., E.S., Y.P.; Supervision, L.H., Y.P., G.G., R.S., W.L.; Investigation, Y.Lobaina., R.C., P.A., A.M., E.S., Y.Lan., M.Z., Z.Z.; Formal analysis, L.H., Y.Lobaina., E.S., Y.P.; Funding acquisition, L.H., K.Y., Y.P., G.G.; Writing—Original Draft, L.H., Y.Lobaina.; Writing—Review & Editing, L.H., Y.Lobaina.; Project administration, L.H., K.Y., W.L., Y.P. All authors reviewed the manuscript.

#### Funding

This work was supported by MOST “National key R&D program of China (2021YFE0192200)”, “PNCT CITMA, Cuba”, “Hunan Provincial Base for Scientific and Technological Innovation Cooperation (2019CB1012)”, “The Science and Technology Innovation Program of Hunan Province, (2020RC5035)”, “Hunan Provincial Innovative Construction Program (2020WK2031).

#### Data Availability

The relevant data is provided within the manuscript. However, considering the large amount of primary data generated, in case that more detailed information is needed, we agree to make it available after specific request.

#### Declarations

##### Ethical approval and consent to participate

The human sera from COVID-19 convalescent and negative individuals were collected at the Eighth- and Ninth-People’s Hospital of Dongguan city (Guangdong Province, China). The study protocol was approved by the Institutional Ethics Committee from both hospitals and was carried out in accordance with the principles of Helsinki declaration. Informed consent was obtained from all donors.

##### Human and animal rights

The studies in mice were conducted at Beijing Vital River Laboratory Animal Technology Co., Ltd, and Hunan Prima Drug Research Center Co., Ltd. Both animal facilities complied with the national standard of the People’s Republic of China GB14925-2010 and the institutional guidelines. Each experimental protocol was subjected to analysis and approval by the Institutional Ethics Committee (Protocols: PANCOV04 approved on 12.04.2022, and HNSE2023(3)012 approved on 20.02.2023). In all the studies inhaled isoflurane, at regular dose or overdose, was employed as anesthesia or euthanasia method, respectively.

##### Competing interests

Y. Lobaina, A.M., P.A., R.C., E.S., Y. Lan, G.C., R.S., G.G., K.Y., Y.P., L.H., are authors of a patent (recently presented in China) related to the content of the manuscript.

Received: 15 July 2024 Accepted: 18 November 2024

Published online: 29 November 2024

#### References

- Cao T, Lazdina U, Desombere I, Vanlandschoot P, Milich DR, Sällberg M, Leroux-Roels G. Hepatitis B virus core antigen binds and activates naive human B cells in vivo: studies with a human PBL-NOD/SCID mouse model. *J Virol*. 2001;75(14):6359–66. <https://doi.org/10.1128/JVI.75.14.6359-6366.2001>.
- Milich DR, Chen M, Schödel F, Peterson DL, Jones JE, Hughes JL. Role of B cells in antigen presentation of the hepatitis B core. *Proc Natl Acad Sci U S A*. 1997;94(26):14648–53. <https://doi.org/10.1073/pnas.94.26.14648>.
- Seeger C, Mason WS. Molecular biology of hepatitis B virus infection. *Virology*. 2015;479–480:672–86.
- Lazdina U, Cao T, Steinbergs J, Alheim M, Pumpens P, Peterson DL, Milich DR, Leroux-Roels G, Sällberg M. Molecular basis for the interaction of the hepatitis B virus core antigen with the surface immunoglobulin receptor on naive B cells. *J Virol*. 2001;75(14):6367–74. <https://doi.org/10.1128/JVI.75.14.6367-6374.2001>.
- Lazdina U, Alheim M, Nyström J, Hultgren C, Borisova G, Sominskaya I, Pumpens P, Peterson DL, Milich DR, Sällberg M. Priming of cytotoxic T cell responses to exogenous hepatitis B virus core antigen is B cell dependent. *J Gen Virol*. 2003;84(Pt 1):139–46. <https://doi.org/10.1099/vir.0.18678-0>.
- Riedl P, Buschle M, Reimann J, Schirmbeck R. Binding immune-stimulating oligonucleotides to cationic peptides from viral core antigen enhances their potency as adjuvants. *Eur J Immunol*. 2002;32(6):1709–16. [https://doi.org/10.1002/1521-4141\(200206\)32:6%3c1709::AID-IMMU1709%3e3.0.CO;2-D](https://doi.org/10.1002/1521-4141(200206)32:6%3c1709::AID-IMMU1709%3e3.0.CO;2-D).
- Vanlandschoot P, Cao T, Leroux-Roels G. The nucleocapsid of the hepatitis B virus: a remarkable immunogenic structure. *Antiviral Res*. 2003;60(2):67–74. <https://doi.org/10.1016/j.antiviral.2003.08.011>.
- Francis MJ, Hastings GZ, Brown AL, Grace KG, Rowlands DJ, Brown F, Clarke BE. Immunological properties of hepatitis B core antigen fusion proteins. *Proc Natl Acad Sci USA*. 1990;87(7):2545–9. <https://doi.org/10.1073/pnas.87.7.2545>.
- Pumpens P, Grens E. HBV core particles as a carrier for B cell/T cell epitopes. *Intervirology*. 2001;44(2–3):98–114. <https://doi.org/10.1159/000050037>.
- Zhang GG, Li DX, Zhang HH, Zeng YM, Chen L. Enhancement of mucosal immune response against the M2eHbc+ antigen in mice with the fusion expression products of LTb and M2eHbc+ through mucosal immunization route. *Vet Res Commun*. 2009;33(7):735–47. <https://doi.org/10.1007/s11259-009-9222-7>.
- Sazegari S, Akbarzadeh Niaki M, Afsharifar A, et al. Chimeric hepatitis B core virus-like particles harboring SARS-CoV2 epitope elicit a humoral immune response in mice. *Microb Cell Fact*. 2023;22:39. <https://doi.org/10.1186/s12934-023-02043-z>.
- Krastina D, Petrovskis I, Petraityte R, Sominskaya I, Ose V, Lieknina I, Bogans J, Sasnauskas K, Pumpens P. Chimeric derivatives of hepatitis B virus core particles carrying major epitopes of the rubella virus E1 glycoprotein. *Clin Vaccine Immunol*. 2013;20(11):1719–28. <https://doi.org/10.1128/CVI.00533-13>.
- Koletzki D, Lundkvist A, Sjölander KB, Gelderblom HR, Niedrig M, Meisel H, Krüger DH, Ulrich R, Puumala (PUU) hantavirus strain differences and insertion positions in the hepatitis B virus core antigen influence B-cell immunogenicity and protective potential of core-derived particles. *Virology*. 2000;276(2):364–75. <https://doi.org/10.1006/viro.2000.0540>.
- Yang M, Lai H, Sun H, et al. Virus-like particles that display Zika virus envelope protein domain III induce potent neutralizing immune responses in mice. *Sci Rep*. 2017;7:7679. <https://doi.org/10.1038/s41598-017-08247-9>.
- Dutta NK, Mazumdar K, Gordy JT. The nucleocapsid protein of SARS-CoV-2: a target for vaccine development. *J Virol*. 2020;94:e00647–e720. <https://doi.org/10.1128/JVI.00647-20>.
- Matchett WE, Vineet Joag J, Stolley M, Shepherd FK, Quarnstrom CF, Mickelson CK, Wijeyesinghe S, Soerens AG, Becker S, Thiede JM, Weyu E, O’Flanagan SD, Walter JA, Vu MN, Menachery VD, Bold TD, Vezys V, Jenkins MK, Langlois RA, Masopust D. Cutting edge: nucleocapsid vaccine elicits spike-independent sars-cov-2 protective immunity. *J Immunol*. 2021;207(2):376–9. <https://doi.org/10.4049/jimmunol.2100421>.
- Dangi T, Class J, Palacio N, Richner JM, Penaloza MacMaster P. Combining spike- and nucleocapsid-based vaccines improves distal control of SARS-CoV-2. *Cell Rep*. 2021;36:109664. <https://doi.org/10.1016/j.celrep.2021.109664>.
- Wood WB. Host specificity of DNA produced by *Escherichia coli*: bacterial mutations affecting the restriction and modification of DNA. *J Mol Biol*. 2011;16:118–33.
- Bullock WO, Fernandez JM, Short JMS. XL1-blue: a high efficiency plasmid transforming *recA* *Escherichia coli* strain with beta-galactosidase selection. *Biotechniques*. 1987;5:376–8.
- Lobaina Y, Chen R, Ai P, Yang L, Alvarez-Lajonchere L, Suzarte E, Tan C, Silva R, Jiang Z, Yang K, Perera Y, Hermida L. Cross-reactive profile against two conserved coronavirus antigens in sera from SARS-CoV-2 hybrid and vaccinated immune donors. *Viral Immunol*. 2023;36(3):222–8. <https://doi.org/10.1089/vim.2022.0186>.
- Towbin H, Staehelin T, Golden J. Electrophoretic transfer of protein from polyacrylamide gel to nitrocellulose sheets procedure and some applications. *Proc Natl Acad Sci*. 1979;76:4350–4.
- Lobaina Y, Trujillo H, García D, Gambe A, Chacon Y, Blanco A, Aguilar JC. The effect of the parenteral route of administration on the immune

- response to simultaneous nasal and parenteral immunizations using a new HBV therapeutic vaccine candidate. *Viral Immunol.* 2010;23:521–9. <https://doi.org/10.1089/vim.2010.0024>.
23. Kundu R, Narean JS, Wang L, Fenn J, Pillay T, Fernandez ND, Conibear E, Koycheva A, Davies M, Tolosa-Wright M, Hakki S, Varro R, McDermott E, Hammett S, Cutajar J, Thwaites RS, Parker E, Rosadas C, McClure M, Tedder R, Taylor GP, Dunning J, Lalvani A. Cross-reactive memory T cells associate with protection against SARS-CoV-2 infection in COVID-19 contacts. *Nat Commun.* 2022;13(1):80. <https://doi.org/10.1038/s41467-021-27674-x>.
  24. Ferretti AP, Kula T, Wang Y, Nguyen DMV, Weinheimer A, Dunlap GS, Xu Q, Nabils N, Perullo CR, Cristofaro AW, Whitton HJ, Virbasius A, Olivier KJ Jr, Buckner LR, Alistar AT, Whitman ED, Bertino SA, Chattopadhyay S, MacBeath G. Unbiased screens show CD8+ T cells of COVID-19 patients recognize shared epitopes in SARS-CoV-2 that largely reside outside the spike protein. *Immunity.* 2020;53(5):1095–107.e3. <https://doi.org/10.1016/j.immuni.2020.10.006>.
  25. Peng Y, Mentzer AJ, Liu G, Yao X, Yin Z, Dong D, Dejnirattisai W, Rostron T, Supasa P, Liu C, López-Camacho C, Slon-Campos J, Zhao Y, Stuart DI, Paesen GC, Grimes JM, Antson AA, Bayfield OW, Hawkins DEDP, Ker DS, Wang B, Turtle L, Subramaniam K, Thomson P, Zhang P, Dold C, Ratcliff J, Simmonds P, de Silva T, Sopp P, Wellington D, Rajapaksa U, Chen YL, Salio M, Napolitani G, Paes W, Borrow P, Kessler BM, Fry JW, Schwabe NF, Semple MG, Baillie JK, Moore SC, Openshaw PJM, Ansari MA, Dunachie S, Barnes E, Frater J, Kerr G, Goulder P, Lockett T, Levin R, Zhang Y, Jing R, Ho LP. Broad and strong memory CD4+ and CD8+ T cells induced by SARS-CoV-2 in UK convalescent individuals following COVID-19. *Nat Immunol.* 2020;21(11):1336–45. <https://doi.org/10.1038/s41590-020-0782-6>.
  26. Tarke A, Sidney J, Kidd CK, Dan JM, Ramirez SJ, Yu ED, Mateus J, da Silva AR, Moore E, Rubiro P, Methot N, Phillips E, Mallal S, Frazier A, Rawlings SA, Greenbaum JA, Peters B, Smith DM, Crotty S, Weiskopf D, Grifoni A, Sette A. Comprehensive analysis of T cell immunodominance and immunoprevalence of SARS-CoV-2 epitopes in COVID-19 cases. *Cell Rep Med.* 2021;2(2):100204. <https://doi.org/10.1016/j.xcrm.2021.100204>.
  27. Lobaina Y, Palenzuela D, Pichardo D, Muzio V, Guillén G, Aguilar JC. Immunological characterization of two hepatitis B core antigen variants and their immunoenhancing effect on co-delivered hepatitis B surface antigen. *Mol Immunol.* 2005;42(3):289–94. <https://doi.org/10.1016/j.molimm.2004.09.005>.
  28. Beterams G, Böttcher B, Nassal M. Packaging of up to 240 subunits of a 17 kDa nuclease into the interior of recombinant hepatitis B virus capsids. *FEBS Lett.* 2000;481(2):169–76. [https://doi.org/10.1016/s0014-5793\(00\)01927-x](https://doi.org/10.1016/s0014-5793(00)01927-x).
  29. Yoshikawa A, Tanaka T, Hoshi Y, Kato N, Tachibana K, Iizuka H, Machida A, Okamoto H, Yamasaki M, Miyakawa Y, et al. Chimeric hepatitis B virus core particles with parts or copies of the hepatitis C virus core protein. *J Virol.* 1993;67(10):6064–70. <https://doi.org/10.1128/JVI.67.10.6064-6070.1993>.
  30. Lopez M, et al. Characterization of the size distribution and aggregation of virus-like nanoparticles used as active ingredients of the HeberNasvac therapeutic vaccine against chronic hepatitis B Adv. Nat Sci Nanosci Nanotechnol. 2017;8:025009. <https://doi.org/10.1088/2043-6254/aa5e1d>.
  31. Riedl P, Stober D, Oehninger C, Melber K, Reimann J, Schirmbeck R. Priming Th1 immunity to viral core particles is facilitated by trace amounts of RNA bound to its arginine-rich domain. *J Immunol.* 2002;168:4951–9.
  32. Chen CY, Chang CK, Chang YW, Sue SC, Bai HJ, Rieng L, et al. Structure of the SARS coronavirus nucleocapsid protein RNA-binding dimerization domain suggests a mechanism for helical packaging of viral RNA. *J Mol Biol.* 2007;368(4):1075–86. <https://doi.org/10.1016/j.jmb.2007.02.06>.
  33. Lobaina Y, Chen R, Suzarte E, Ai P, Huerta V, Musacchio A, Silva R, Tan C, Martín A, Lazo L, et al. The nucleocapsid protein of SARS-CoV-2, combined with ODN-39M, is a potential component for an intranasal bivalent vaccine with broader functionality. *Viruses.* 2024;16:418. <https://doi.org/10.3390/v16030418>.
  34. van Beek LF, den van Langereis JD, Berg van Saparoea HB, Gillard J, Jong WSP, van Opzeeland FJ, Mesman R, van Niftrik L, Joosten I, Diavatopoulos DA, et al. Intranasal vaccination with protein bodies elicit strong protection against streptococcus pneumoniae colonization. *Vaccine.* 2021;39:6920–9. <https://doi.org/10.1016/j.vaccine.2021.10.006>.
  35. Bode C, Zhao G, Steinhagen F, Kinjo T, Klinman DM. CpG DNA as a vaccine adjuvant. *Expert Rev Vaccines.* 2011;10:499–511. <https://doi.org/10.1586/erv.10.174>.
  36. Scheiermann J, Klinman DM, Klinman D. Vaccines targeting infectious diseases and cancer. *Pharmaceutics.* 2015;13(2):142.
  37. Gil L, Marcos E, Izquierdo A, Lazo L, Valdés I, Ambala P, Ochola L, Hitler R, Suzarte E, Álvarez M, et al. The protein DIIIc-2, aggregated with a specific oligodeoxynucleotide and adjuvanted in alum, protects mice and monkeys against DENV-2. *Immunol Cell Biol.* 2015;93:57–66. <https://doi.org/10.1038/icb.2014.63>.
  38. Gil L, Cobas K, Lazo L, Marcos E, Hernández L, Suzarte E, Izquierdo A, Valdés I, Blanco A, Puentes P, et al. A tetravalent formulation based on recombinant nucleocapsid-like particles from dengue viruses induces a functional immune response in mice and monkeys. *J Immunol.* 2016;197:3597–606. <https://doi.org/10.4049/jimmunol.1600927>.
  39. Olivera S, Perez A, Falcon V, Urquiza D, Pichardo D, Martínez-Donato G. Protective cellular immune response against hepatitis c virus elicited by chimeric protein formulations in BALB/c Mice. *Arch Virol.* 2020;165:593–607. <https://doi.org/10.1007/s00705-019-04464-x>.
  40. McMahan K, Yu J, Mercado NB, Loos C, Tostanoski LH, Chandrashekar A, Liu J, Peter L, Atyeo C, Zhu A, Bondzie EA, Dagotto G, Gebre MS, Jacob-Dolan C, Li Z, Nampanya F, Patel S, Pessaint L, Van Ry A, Blade K, Yalley-Ogunro J, Cabus M, Brown R, Cook A, Teow E, Andersen H, Lewis MG, Lauffenburger DA, Alter G, Barouch DH. Correlates of protection against SARS-CoV-2 in rhesus macaques. *Nature.* 2021;590(7847):630–4. <https://doi.org/10.1038/s41586-020-03041-6>.
  41. Yu H, Guan F, Miller H, Lei J, Liu C. The role of SARS-CoV-2 nucleocapsid protein in antiviral immunity and vaccine development. *Emerg Microb Infect.* 2023;12:e2164219. <https://doi.org/10.1080/22221751.2022.2164219>.
  42. Dangi T, Sanchez S, Class J, Richner M, Visvabharathy L, Chung YR, Bentley K, Stanton RJ, Koralnik IJ, Richner JM, Penaloza-MacMaster P. Improved control of SARS-CoV-2 by treatment with a nucleocapsid-specific monoclonal antibody. *J Clin Invest.* 2022;132(23):e162282. <https://doi.org/10.1172/JCI162282>.
  43. Herman JD, Wuang C, Burke JS, Zur Y, Compere H, Kang J, Macvicar R, Shin S, Frank I, Siegel D, Tebas P, Choi GH, Shaw PA, Yoon H, Liise-anne Pirofski L-A, Juelg B, Bar KJ, Lauffenburger D, Alter G. A role for Nucleocapsid-specific antibody function in Covid-19 Convalescent plasma therapy (preprint). medRxiv. 2022. <https://doi.org/10.1101/2022.02.19.22271230>.
  44. Gromowska GD, Macedo-Cincotta C, Mayer S, King J, Swafford I, McCracken MK, Coleman D, Enoch J, Storme C, Darden J, Peel S, Epperson D, McKee K, Currier JK, Okuliczi J, Paquin-Proulx D, Cowden J, Peachman B. Humoral immune responses associated with control of SARS-CoV-2 breakthrough infections in a vaccinated US military population. *eBioMedicine.* 2023;94:104683. <https://doi.org/10.1016/j.ebiom.2023.104683>.
  45. Zhuang Z, Lai X, Sun J, Chen Z, Zhang Z, Dai J, Liu D, Li Y, Li F, Wang Y, et al. Mapping and role of T cell response in SARS-CoV-2-infected mice. *J Exp Med.* 2021;218:e20202187. <https://doi.org/10.1084/jem.20202187>.
  46. Tilocca B, Soggiu A, Sanguinetti M, Musella V, Britti D, Bonizzi L, Urbani A, Roncada P. Comparative computational analysis of SARS-CoV-2 nucleocapsid protein epitopes in taxonomically related coronaviruses. *Microbes Infect.* 2020;22:188–94. <https://doi.org/10.1016/j.micinf.2020.04.002>.
  47. Ravelomanantsoa NAF, Guth S, Andrianiaina A, Andry S, Gentles A, Ranaivoson HC, Brook CE. The zoonotic potential of bat-borne coronaviruses. *Emerg Top Life Sci.* 2020;4:353–69. <https://doi.org/10.1042/ETLS20200097>.
  48. Crook JM, Murphy I, Carter DP, Pullan ST, Carroll M, Vipond R, Cunningham AA, Bell D. Metagenomic Identification of a New Sarbecovirus from Horseshoe Bats in Europe. *Sci Rep.* 2021;11:14723. <https://doi.org/10.1038/s41598-021-94011-z>.
  49. Maini MK, Boni C, Lee CK, Larrubia JR, Reignat S, Ogg GS, King AS, Herberg J, Gilson R, Alisa A, Williams R, Vergani D, Naoumov NV, Ferrari C, Bertoletti A. The role of virus-specific CD8(+) cells in liver damage and viral control during persistent hepatitis B virus infection. *J Exp Med.* 2000;191(8):1269–80. <https://doi.org/10.1084/jem.191.8.1269>.
  50. Webster GJ, Reignat S, Brown D, Ogg GS, Jones L, Seneviratne SL, Williams R, Dusheiko G, Bertoletti A. Longitudinal analysis of CD8+ T cells specific for structural and nonstructural hepatitis B virus proteins in patients with chronic hepatitis B: implications for immunotherapy. *J Virol.* 2004;78(11):5707–19. <https://doi.org/10.1128/JVI.78.11.5707-5719.2004>. PMID:15140968;PMCID:PMC415806.

51. Aguiar JA, Marrero MA, Figueroa DA, Aguilar A, Idavoy A, Martinez S, Moran I, et al. Preparing for the next pandemic: increased expression of interferon-stimulated genes after local administration of nasalferon or hebernasvac. *DNA Cell Biol.* 2024;43(2):283. <https://doi.org/10.1089/dna.2023.0283>.

### **Publisher's Note**

Springer Nature remains neutral with regard to jurisdictional claims in published maps and institutional affiliations.